# Main Manuscript for

# Epistasis is not a strong constraint on the recurrent evolution of toxin-resistant $Na^+$,$K^+$-ATPases among tetrapods.

Shabnam Mohammadi[1,2,*], Lu Yang[3, §,*], Santiago Herrera-Álvarez[4,5,*], María del Pilar Rodríguez-Ordoñez[4,#], Karen Zhang[3], Jay F. Storz[1], Susanne Dobler[2], Andrew J. Crawford[4] & Peter Andolfatto[6]

[1]School of Biological Sciences, University of Nebraska, Lincoln, NE, USA
[2]Molecular Evolutionary Biology, Institute of Zoology, Biocenter Grindel, Universität Hamburg, Hamburg, Germany
[3]Department of Ecology and Evolution, Princeton University, Princeton, NJ, USA
[4]Department of Biological Sciences, Universidad de los Andes, Bogotá, 111711, Colombia
[5]Department of Ecology and Evolution, University of Chicago, Chicago, IL, USA
[6]Department of Biological Sciences, Columbia University, New York, NY, USA

*Co-first authorship

[§] Current address: Wellcome Sanger Institute, Cambridge, United Kingdom
[#] Current address: Université Paris-Saclay Evry, Evry, France

**Email:** andrew@dna.ac, pa2543@columbia.edu

SM: 0000-0003-3450-6424, LY: 0000-0002-2694-1189, SHA: 0000-0002-0793-7811, MPRO: 0000-0002-0856-1297, KZ: 0000-0003-4406-9977, JFS: 0000-0001-5448-7924, SD: 0000-0002-0635-7719, AJC: 0000-0003-3153-6898, PA: 0000-0003-3393-4574

**Classification**
Biological Sciences; Evolution

**Keywords**
Epistasis, protein evolution, cardiotonic steroids, toxin resistance, adaptation

**Author Contributions**
PA and AJC conceived of and oversaw the project; SM, JFS, SD, AJC and PA designed experiments; KZ, LY, MPRO, SHA, SM collected data; SM, SHA and PA performed evolutionary and statistical analyses; SM, SHA, and PA wrote the paper; All authors edited the manuscript.

**This PDF file includes:**
Main Text
Figures 1 to 6

**Abstract**

Comparative genomic studies reveal a global decline in rates of convergent amino acid substitution as a function of evolutionary distance. This pattern has been attributed to epistatic constraints on protein evolution, the idea being that mutations tend to confer the same fitness effects on more similar genetic backgrounds, so convergent substitutions are more likely to occur in closely related species. However, this hypothesis lacks experimental validation. We tested this model in the context of the recurrent evolution of resistance to cardiotonic steroids (CTS) across diverse groups of tetrapods, which occurs via specific amino acid substitutions to the α-subunit family of $Na^+$,$K^+$-ATPases (ATP1A). After identifying a series of recurrent substitutions at two key sites of ATP1A1 predicted to confer CTS resistance, we performed protein engineering experiments to test the functional consequences of introducing these substitutions onto divergent species backgrounds. While we find that substitutions at these sites can have substantial background-dependent effects on CTS resistance, we also find no evidence for background-dependent effects on protein activity. We further show that the magnitude of a substitution's effect on activity does not depend on the overall extent of ATP1A1 sequence divergence between species. More generally, a global analysis of substitution patterns across ATP1A orthologs and paralogs reveals that the probability of convergent substitution protein-wide is not predicted by sequence divergence. Together, these findings suggest that intramolecular epistasis is not an important constraint on the evolution of ATP1A CTS resistance in tetrapods.

**Significance Statement**

Individual amino acid residues within a protein work in concert to produce a functionally coherent structure that must be maintained even as orthologous proteins in different species diverge over time. Given this dependence, we expect identical mutations to have more similar effects on protein function in more closely related species. We tested this hypothesis by performing protein-engineering experiments on ATP1A, an enzyme mediating target-site insensitivity to cardiotonic steroids (CTS) in diverse animals. These experiments reveal that although the phenotypic effects of substitutions can sometimes be background-dependent, the magnitude of these effects does not correlate with ATP1A1 sequence divergence. This implies that the genetic background across the ATP1A protein does not strongly limit the evolution of CTS resistance in animals.

## Main Text

## Introduction

Patterns of molecular parallelism and convergence represent a useful paradigm to examine the factors that limit the rate of adaptation and the extent to which adaptive evolutionary paths are predictable (1, 2). In the context of protein evolution, patterns of parallelism and convergence are influenced by pleiotropy (the effect of a given mutation on multiple phenotypes) and intramolecular epistasis (nonadditive interactions between mutant sites in the same protein) (3–11). If the phenotypic and fitness effects of mutations depend on the genetic background on which they arise (i.e. epistasis), a given mutation is expected to have more similar effects in orthologs from closely related species. Therefore, the probability of parallel or convergent substitution resulting in sequence divergence between species is expected to decrease with divergence time. Consistent with this expectation, there is evidence for such a decline in broad-scale phylogenetic comparisons of mitochondrial (12) and nuclear (13, 14) proteins. However, this hypothesis has not been tested experimentally to date.

To address the question of how changes in the genetic background alter the phenotypic effects of new mutations, we focus on the test case of the repeated evolution of resistance to cardiotonic steroids (CTS) in animals. CTS are potent inhibitors of $Na^+$,$K^+$-ATPase (NKA), a protein that plays a critical role in maintaining membrane potential and is consequently vital for the maintenance of many physiological processes and signaling pathways in animals (15). NKA (Fig. 1A) is a heterodimeric transmembrane protein that consists of a catalytic α-subunit (ATP1A) and a glycoprotein $\beta$-subunit (ATP1B) (16). CTS inhibit NKA function by binding to a highly conserved domain of ATP1A and blocking the exchange of $Na^+$ and $K^+$ ions (15). NKA is thus often the target of parallel evolution of CTS resistance in insect herbivores that feed on toxic plants (17, 18) as well as vertebrate predators that feed on toxic prey (19–22). Functional investigations of CTS resistance-conferring substitutions in Drosophila (23, 24) and Neotropical grass frogs (25) revealed associated negative pleiotropic effects on protein function and showed that substitutions elsewhere in the protein mitigate these effects. However, despite these examples, the generality of these patterns, and specifically the predicted dependence on evolutionary distance, remain poorly understood given the limited availability of comparative functional data.

Broad phylogenetic comparisons in vertebrates have focused primarily on the H1-H2 extracellular loop of ATP1A proteins, a subset of the CTS-binding domain that contains two sites (111 and 122) known to underlie CTS resistance in rats and toad-eating frogs (25, 26). Most vertebrates possess three paralogs of the α-subunit gene (ATP1A) that have different tissue-specific expression profiles and are associated with distinct physiological roles (Fig. 1B) (15, 27). Mammals possess a fourth

107 paralog that is expressed predominantly in testes (28). A major limitation of studies to date is that
108 the H1-H2 extracellular loop has been inconsistently surveyed among vertebrate taxa, with
109 previous studies focusing on ATP1A3 in reptiles (20, 21, 29, 30), ATP1A1 and/or ATP1A2 in birds
110 and mammals (30, 31), and either ATP1A1 or ATP1A3 in amphibians (19, 30). We therefore lack
111 a comprehensive survey of amino acid variation in the ATP1A protein family across vertebrates.
112
113 To bridge this gap, we first surveyed variation in near full-length coding sequences of the three
114 NKA α-subunit paralogs (ATP1A1, ATP1A2, ATP1A3) that are shared across major extant tetrapod
115 groups (mammals, birds, non-avian reptiles, and amphibians), and identified substitutions that
116 occur repeatedly among divergent lineages. Focusing on two key sites implicated in CTS resistance
117 across animals (111 and 122), we tested whether substitutions at these sites have increasingly
118 distinct phenotypic effects on more divergent genetic backgrounds. Specifically, we engineered
119 several common substitutions at sites 111 and 122 of ATP1A1 that differ between species to reveal
120 potential 'cryptic' epistasis (8, 32). By quantifying the level of CTS resistance conferred by these
121 substitutions, as well as their effects on enzyme function, we evaluate the extent to which pleiotropy
122 and epistasis have constrained the evolution of CTS-resistant forms of ATP1A1 across tetrapods.
123
124
125 **Results**
126
127 **Patterns of ATP1A sequence evolution across species and paralogs.**
128
129 To obtain a more comprehensive portrait of ATP1A amino acid variation among tetrapods, we
130 created multiple sequence alignments for near full-length ATP1A proteins for the three ATP1A
131 paralogs shared among vertebrates. In addition to publicly available data, we generated new RNA-
132 seq data for 27 non-avian reptiles (PRJNA754197) (Table S1-S2). We then *de novo* assembled
133 full-length transcripts of all ATP1A paralogs using these and RNA-seq data from 18 anuran species
134 (25) (PRJNA627222) to achieve better representation for these groups. In total, this dataset
135 comprises 429 species for ATP1A1, 197 species for ATP1A2 and 204 species for ATP1A3 (831
136 sequences total; Supplemental Dataset 1, Fig. S1).
137
138 Our survey reveals numerous substitutions at sites implicated in CTS resistance of NKA (Fig. 2;
139 Supplementary Dataset 2; for comparison to insects, see Supplemental file 1 of ref. (23)). As
140 anticipated from studies of full-length sequences in insects (17, 18, 23), most amino acid variation
141 among species and paralogs is concentrated in the H1-H2 extracellular loop (residues 111-122;
142 Fig 1A). Despite harboring just 28% of 43 sites previously implicated in CTS resistance (33), the

143 H1-H2 extracellular loop contains 81.4% of all substitutions identified among the three ATP1A
144 paralogs (Fig. S2).

145 Our survey reveals several clade- and paralog-specific patterns. Notably, ATP1A1 exhibits more
146 variation among species at sites implicated in CTS resistance (Fig. 2). Most of the variation in
147 ATP1A2 at these sites is restricted to squamate reptiles and ATP1A3 lacks substitutions at site 122
148 altogether, despite the well-known potential for substitutions at this site to confer CTS resistance
149 (25, 26). Looking across species and paralogs, the extent of parallelism at sites 111 and 122 is
150 remarkable (Figs. 2-3): for example, the substitutions Q111E, Q111T, Q111H, Q111L, and Q111V
151 all occur in parallel in multiple species of both insects and vertebrates. N122H and N122D also
152 frequently occur in parallel in both of these major clades. The frequent parallelism of CTS-sensitive
153 (i.e. Q111 and N122) to CTS-resistant states at these sites has been interpreted as evidence for
154 adaptive significance of these substitutions (17–20), but may also reflect mutation biases (34) and
155 the nature of physico-chemico constraints (13, 35).

156 In contrast, some parallelism is restricted to specific clades: for example, Q111R occurs in parallel
157 across tetrapods but has not been observed in insects. Similarly, the combination Q111R+N122D
158 has evolved three times independently in ATP1A1 of tetrapods but is not observed in insects.
159 Conversely, insects have evolved Q111V+N122H independently four times, but this combination
160 has never been observed in tetrapods. These patterns suggest that the fitness effects of some
161 CTS-resistant substitutions depend on genetic background, with the result that CTS-resistance
162 evolved via different mutational pathways in different lineages.

163 Beyond known CTS-resistant substitutions at sites 111 and 122, some taxa have evolved other
164 paths to CTS resistance. For example, the Pacman frog (genus *Ceratophyrs*) is known to prey on
165 CTS-containing toads (36) and its ATP1A1 harbors a known CTS-resistant substitution at site 121
166 (D121N, Supplementary Dataset 2). This substitution is rare among vertebrates but has been
167 previously reported in CTS-adapted milkweed bugs (17, 18). Similarly, the known CTS resistance
168 substitution C104Y is observed among many natricid snakes (Supplementary Dataset 2) and CTS-
169 adapted milkweed weevils (18). Chinchilla (*Chinchilla lanigera*) and yellow-throated sandgrouse
170 (*Pterocles gutturalis*) show distinct single-amino acid insertions in the H1–H2 extracellular loop, a
171 characteristic that has been previously associated with CTS resistance in pyrgomorphid
172 grasshoppers (33, 37). Further, *in lieu* of variation at site 122, ATP1A3 of tetrapods harbors
173 frequent parallel substitutions at site 120 (G120R). Interestingly, this site also shows substantial
174 parallel substitution in the ATP1A1 paralog of birds (where N120K occurs eight times
175 independently) but is mostly invariant in ATP1A1 of other tetrapods.

176

177 **Context-dependent CTS resistance for substitutions at sites 111 and 122**

178

179 The clade- and paralog-specific patterns of substitution among ATP1A paralogs outlined above
180 suggest that the evolution of CTS resistance may be highly dependent on sequence context.
181 However, the functional effects of the vast majority of these substitutions on the diverse genetic
182 backgrounds in which they occur remain largely unknown (25, 26, 29). Given the diversity and
183 broad phylogenetic distribution of parallel substitutions at sites 111 and 122, and the documented
184 effects of some of these substitutions on CTS resistance, we experimentally tested the extent to
185 which functional effects of substitutions at these sites are background-dependent.

186

187 We focused functional experiments on ATP1A1, because it is the most ubiquitously expressed
188 paralog and exhibits both the most sequence diversity and the broadest phylogenetic distribution
189 of parallel substitutions. Specifically, we considered ATP1A1 orthologs from nine representative
190 tetrapod species that possess different combinations of wild-type amino acids at 111 and 122 (Fig.
191 4A). Our taxon sampling includes two lizards, two snakes, two birds, two mammals and previously
192 published data for one amphibian (Fig. S4; Fig. S5; Table S3). The ancestral amino acid states of
193 sites 111 and 122 in tetrapods are Q and N, respectively. We found that the sum of the number of
194 derived states at positions 111 and 122 is a strong predictor of the level of CTS-resistance (Fig 4B,
195 $IC_{50}$, Spearman's $r_S$=0.85, p=0.001). Nonetheless, we also found greater than 10-fold variation in
196 CTS-resistance among enzymes that had identical paired states at 111 and 122 (e.g., compare
197 chinchilla (CHI) versus red-necked keelback snakes (KEE) or compare rat (RAT) versus the
198 resistant paralog of grass frogs ($GRA_R$)). These differences suggest that substitutions at other sites
199 also contribute to CTS resistance.

200

201 To test for epistatic effects of common CTS-resistant substitutions at sites 111 and 122, we used
202 site-directed mutagenesis to introduce 15 substitutions (nine at position 111 and six at position 122)
203 in the wildtype ATP1A1 backgrounds of 9 different species (Fig. S4). The specific substitutions
204 chosen were either phylogenetically broadly-distributed parallel substitutions and/or divergent
205 substitutions that distinguish closely related clades of species. We expressed each of these 24
206 ATP1A1 constructs with an appropriate species-specific ATP1B1 protein (Table S3). For each
207 recombinant NKA protein complex, we characterized its level of CTS resistance ($IC_{50}$) and we
208 estimated enzyme activity as the rate of ATP hydrolysis in the absence of CTS (Table S4).

209

210 Of the 12 substitutions for which $IC_{50}$ could be measured, substitutions had a 15-fold effect on
211 average (Fig. 4C, Table S4) and were equally likely to increase or decrease $IC_{50}$. To assess the

212 background-dependence of specific substitutions, we examined five cases in which a given
213 substitution (e.g., E111H), or the reverse substitution (e.g., H111E), could be evaluated on two or
214 more backgrounds. In the absence of intramolecular epistasis, the effect of a substitution in different
215 backgrounds should remain unchanged and the magnitude of the effect of the reverse substitution
216 should also be the same but with opposite sign. This analysis revealed substantial background
217 dependence for $IC_{50}$ in two of the five informative cases (Fig. 4E; Table S5). In one case, the N122D
218 substitution results in a 200-fold larger increase in $IC_{50}$ when added to the chinchilla (CHI)
219 background compared to the grass frog (GRA) background (p=1.2e-3 by ANOVA). In the other
220 case, the E111H substitution and the reverse substitution (H111E) produced effects in the same
221 direction (reducing CTS-resistance) when added to different backgrounds (false fer-de-lance (FER)
222 and red-necked keelback (KEE) snakes, respectively, p=1e-7 by ANOVA). Overall, these results
223 suggest that the effect of a given substitution on $IC_{50}$ can be strongly dependent on the background
224 on which it occurs. The remaining three substitutions (H111T, Q111R and H122D) showed no
225 significant change in the magnitude of the effect on $IC_{50}$ when introduced into different species'
226 backgrounds. These results suggest that, while some substitutions can have strong background-
227 dependent effects, strong intramolecular epistasis with respect to CTS resistance is not universal.
228
229 **Pleiotropic effects on NKA activity exhibit little evidence for background-dependence.**
230
231 We next tested whether substitutions at sites 111 and 122 have pleiotropic effects on ATPase
232 activity. Because ion transport across the membrane is a primary function of NKA and its disruption
233 can have severe pathological effects (38), mutations that compromise this function are likely to be
234 under strong purifying selection. As suggested by previous work (23–25), CTS-resistant
235 substitutions at sites 111 and 122 can decrease enzyme activity. We evaluated the generality of
236 these effects by comparing enzyme activity of the 15 mutant NKA proteins to their corresponding
237 wild-type proteins.
238
239 Interestingly, the wild-type enzymes themselves exhibit substantial variation in activity, from 3-18
240 nmol/mg*min (*P* = 6e-7 by ANOVA, Fig 4D; Table S4). On average, substitutions at sites 111 and
241 122 changed enzyme activity by 60% (Fig 4D; Fig S4). In two cases, amino acid substitutions at
242 position 122 (N122H and H122D) nearly inactivate lizard NKAs and, in one case, a substitution at
243 position 111 (Q111T) resulted in low expression of the recombinant protein in the transfected cells
244 (Fig S5; Fig. S6). A test of uniformity of pairwise t-test p-values across substitutions suggests a
245 significant enrichment of low p-values (Fig 4D inset; p=2.5e-4, chi-squared test of uniformity). Thus,
246 globally, this set of substitutions has significant effects on NKA activity, but they were not

247 significantly more likely to decrease than increase activity (10 decrease: 5 increase, p>0.3, binomial
248 test, Fig. 4D, Table S5).
249
250 We next asked to what extent pleiotropic effects of CTS resistant substitutions at positions 111 and
251 122 are dependent on genetic background. This question is motivated by recent studies in insects
252 which revealed that deleterious pleiotropic effects of some resistance-conferring substitutions at
253 sites 111 and 122 are background-dependent (23, 24). Likewise, recent work on ATP1A1 of toad-
254 eating grass frogs showed that effects of Q111R and N122D on NKA activity are background-
255 dependent (25). In contrast, among the five informative cases in which we compared the same
256 substitution (or the reverse substitution) on two or more backgrounds, there is little evidence for
257 background dependence (Fig 4E; Table S5). For example, N122D has similar effects on NKA
258 activity in grass frog and chinchilla despite the substantial divergence between the species' proteins
259 (8.4% protein sequence divergence; Fig. 4D). Similarly, the effects of Q111R in ostrich or the
260 reverse substitution R111Q in sandgrouse were not significantly different from the effect of Q111R
261 in grass frog (7.5% and 8% protein sequence divergence, respectively).
262
263 To further examine the evidence for background dependence, we tested whether changes to the
264 same amino acid state (regardless of starting state) at 111 and 122 produce different changes in
265 NKA activity (e.g., R111E on the rat background versus H111E on the false fer-de-lance
266 background). If epistasis is important, we expect that the difference in effects of substitutions to a
267 given amino acid state should increase with increasing sequence divergence compared to ATP1A1
268 backgrounds in which that state is wild-type. However, across the 11 possible comparisons, we
269 found no relationship between the difference in the effect of substitutions to the same state and the
270 extent of amino acid divergence between the orthologous proteins (Fig. 5). This pattern suggests
271 that, while pleiotropic effects can be background dependent (23, 25), these effects are not
272 pervasive across species and do not correlate with overall sequence divergence.
273
274
275 **The overall rate of convergence across ATP1A proteins does not depend on sequence**
276 **divergence.**
277
278 If intramolecular epistasis is pervasive, we would predict that rates of convergent substitution
279 should decrease as a function of overall sequence divergence (12–14). In contrast to this
280 expectation, our experiments suggest that, for ATP1A1, the extent of background sequence
281 divergence is a poor predictor of the magnitude of effects of substitutions at sites 111 and 122 on
282 CTS resistance and enzyme activity. Since our experiments were necessarily limited in scope, we

283 carried out a broad phylogenetic analysis to evaluate how well our findings align with global
284 estimates of rates of convergence for the ATP1A family beyond ATP1A1 and beyond sites
285 implicated in CTS resistance.
286
287 Using a multisequence alignment of 831 ATP1A protein sequences, including the three ATP1A
288 paralogs shared among tetrapods (i.e., amphibians, non-avian reptiles, birds, and mammals), we
289 inferred a maximum likelihood phylogeny of the gene family (Fig. S1). We then used ancestral
290 sequence reconstruction to infer the history of substitution events on all branches in the tree and
291 counted the number of convergent amino acid substitutions along the protein per site (see Materials
292 and Methods). Convergent substitutions are defined as substitutions on two branches at the same
293 site resulting in the same amino acid state. Interestingly, we do not detect a correlation between
294 the relative number of convergent substitutions with background ATP1A divergence across the tree
295 (Fig. 6A). This result also holds true when considering only substitutions to the key CTS resistance
296 sites 111 and 122 (Fig. S5).
297
298 To gain more insight into the factors that determine convergent evolution in ATP1A, we looked
299 more closely at patterns of individual convergent substitutions at sites 111 and 122 by extracting
300 each convergent substitution and visualizing its distribution along the sequence divergence axis
301 (Fig. 6B). Under the expectation that rates of convergence should tend to decrease as a function
302 of sequence divergence, the distribution of pairwise convergent events along the sequence
303 divergence axis should be left-skewed, with a peak towards lower sequence divergence. In contrast
304 to this expectation, the distribution is bimodal, with one peak at 0.33 and the other at 0.69
305 substitutions/site (Fig. 6B bottom panel). Parallel and convergent substitutions have occurred
306 almost across the full range of protein divergence estimates. For example, if X is any starting state,
307 the substitution X111R has occurred independently in 13 tetrapod lineages and X111L
308 independently in 20 lineages. Both substitutions have a broad phylogenetic distribution, suggesting
309 that their effects do not strongly depend on overall genetic background. Interestingly, however, the
310 distributions for X111H and X111E substitutions are relatively right-skewed, in line with epistasis
311 for CTS resistance that we observed in experiments for H111E/E111H (Fig 4E). Overall, the results
312 of these analyses align well with our functional experiments but run contrary to expectations based
313 on previously reported proteome-wide evolutionary trends (12–14).
314
315 **Discussion**
316
317 Previous work has suggested that rates of convergent amino-acid substitution generally decline as
318 a function of time, a pattern that can potentially be explained by epistatic constraints. According to

319 this view, the higher the level of sequence divergence between a given pair of homologs, the higher
320 the probability that the same mutation will have different fitness effects on the two backgrounds
321 (12). In that respect, our broad survey of the ATP1A gene family in tetrapods, in combination with
322 previous work, reveals two striking and seemingly contradictory patterns. The first is that some
323 substitutions underlying CTS resistance in tetrapods are broadly distributed phylogenetically and
324 even shared with insects (e.g., N122H is widespread among snakes and found in the monarch
325 butterfly and other insects; see Fig. 3 for more examples). Patterns like these suggest that epistatic
326 constraints have a limited role in the evolution of CTS resistance, as the same mutation can be
327 favored on highly divergent genetic backgrounds. On the other hand, there is also substantial
328 diversity in resistance-conferring states at sites 111 and 122, and some combinations of these
329 substitutions appear to be phylogenetically restricted. For example, the CTS-resistant combination
330 of Q111R+N122D has evolved multiple times in tetrapods but is absent in insects, whereas the
331 CTS-resistant combination Q111V+N122H evolved multiple times in insects but is absent in
332 tetrapods (Fig 3). Additionally, some substitutions also appear to be paralog-specific in tetrapods
333 (Fig 3). These phylogenetic signatures suggest at least some role for epistasis as a source of
334 contingency in the evolution of ATP1A-mediated CTS resistance in animals (i.e., the fitness effects
335 of substitutions depend on the order in which they occur). How can these disparate patterns be
336 reconciled? To what extent do genetic background and contingency limit the evolution of CTS
337 resistance in animals?
338
339 In our survey of putative CTS-resistant substitutions at sites 111 and 122, we find that derived
340 substitutions have largely predictable effects on CTS resistance, with notable exceptions that tend
341 to be in magnitude rather than direction (Fig. 4C and 4E). While derived states at sites 111 and 122
342 are generally a reliable predictor of CTS resistance (Fig. 4A), they do not always predict the effect
343 size of particular substitutions (e.g., Q111R contributes to CTS resistance on many species'
344 backgrounds, but not on that of sandgrouse, Fig. 4C). It is also notable that species with identical
345 paired states at 111 and 122 can vary in CTS resistance by more than an order of magnitude. Both
346 patterns point to background determinants of CTS resistance that may be additive rather than
347 epistatic. Yet there are some broadly phylogenetically distributed substitutions, such as N122D,
348 that nonetheless do exhibit background-dependent effects on CTS resistance (Fig. 4C and 4E).
349
350 While epistasis is likely to be a pervasive feature in protein evolution, many mutational effects on
351 structural and functional properties of proteins appear to be purely additive (e.g., (39–41). In line
352 with this, our experimental results revealed that the phenotypic effects of individual substitutions
353 on ATPase activity are likely to be additive in general. We also found no correlation between the
354 marginal effect of a substitution with background genetic divergence. Specifically, mutating to the

355 same amino acid state (irrespective of the initial state) doesn't result in larger effects in more distant
356 backgrounds. Under additivity, the rate of convergence is expected to be uncorrelated with
357 background genetic distance because the phenotypic effect of a mutation does not depend on the
358 amino acid states at other sites in the protein. Our phylogenetic and experimental results align with
359 this expectation.
360
361 While the extent to which changes in CTS resistance are favorable to an organism depend on
362 physiological constraints and the specific ecological context (e.g., in which tissues NKA is
363 expressed and the presence of dietary CTS), changes in enzyme activity associated with these
364 substitutions are most likely detrimental to organismal fitness. It follows that changes to the ATP1A1
365 background would be required to offset such changes in enzyme activity. Surprisingly, we found
366 that, with rare exceptions, CTS-resistant substitutions at sites 111 and 122 tend to exhibit little or
367 no pleiotropy with respect to enzyme activity. In addition, amino acid substitutions were not
368 significantly more likely to decrease rather than increase activity. Interestingly, the activity of
369 wildtype ATP1A1 enzymes varies 6-fold among the species surveyed (Fig. 4E), suggesting that
370 most species are either robust to changes in NKA activity, or that changes have occurred in other
371 genes (including other ATP1A paralogs) that compensate for changes in activity. Thus, it may be
372 that protein activity itself is either not an important pleiotropic constraint on the evolution of ATP1A
373 CTS resistance or that constraint depends not just on the protein background, but also on the
374 background at higher levels (e.g., other interacting proteins). A further possibility is that detrimental
375 effects of CTS resistant substitutions depend on few sites, and these sites are also highly
376 convergent (e.g., A119S among insect herbivores, see refs. 23 and 24).
377
378 We conclude that intramolecular epistasis in ATP1A -- at the level of protein activity -- is unlikely to
379 represent a substantial constraint in the evolution of CTS resistance. However, the lack of evidence
380 of epistasis at the level of protein function does not preclude an important role for epistasis at higher
381 levels. For example, our results are also consistent with a scenario of nonspecific (or global)
382 epistasis, where mutations have additive effects on molecular phenotypes (e.g., ATPase activity)
383 but have nonadditive effects on fitness due to a nonlinear relationship between phenotype and
384 fitness (7, 40, 42). Nonspecific epistasis predicts a many-to-one relationship with respect to genetic
385 backgrounds and specific mutations (7, 42), such that many genetic backgrounds can compensate
386 for the deleterious effects of a given mutation. Thus, nonspecific epistasis of this form could explain
387 why CTS resistant substitutions at sites 111 and 122 exhibit broad phylogenetic distributions.
388
389 Dependence on few sites, or the many-to-one nature of non-specific epistasis, may also account
390 for the weak signature of decreasing convergence with increasing divergence for ATP1A. Our study

391 suggests that, while intramolecular epistasis may be pervasive across proteomes, it does not
392 always represent a substantial constraint on the evolution of adaptive traits, as we show here for
393 CTS resistance in tetrapods. Further evaluation of epistasis at higher levels than enzyme activity
394 (e.g., whole organism neural function, CTS tolerance or viability, refs. 23, 24) may elucidate the
395 extent to which nonspecific epistasis constrains protein evolution in these cases.
396

397 **Materials and Methods**

398

399 **Sample collection and data sources.**

400 In order to carry out a comprehensive survey of vertebrate ATP1A paralogs, we collated a total of
401 831 protein sequences for this study (Supplementary Dataset 1). In addition to publicly available
402 data, we also generated RNA-seq data for 27 species of non-avian reptiles (Table S1;
403 PRJNA754197) to achieve a better representation of some previously underrepresented lineages.
404 These included field-caught and museum-archived specimens as well as animals purchased from
405 commercial pet vendors. Purchased animals were processed following the procedures specified in
406 the IACUC Protocol No. 2057-16 (Princeton University) and implemented by a research
407 veterinarian at Princeton University. Wild-caught animals were collected under Colombian umbrella
408 permit *resolución No*. 1177 granted by the *Autoridad Nacional de Licencias Ambientales* to the
409 Universidad de los Andes and handled according to protocols approved by the Institutional
410 Committee on the Care and Use of Laboratory Animals (abbreviated CICUAL in Spanish) of the
411 Universidad de los Andes. In all cases, fresh tissues (brain, stomach, and muscle) were taken and
412 preserved in RNAlater (Invitrogen) and stored at -80ºC until used.

413

414 **Reconstruction of ATP1A paralogs.**

415 RNA-seq libraries were prepared either using TruSeq RNA Library Prep Kit v2 (Illumina) and
416 sequenced on Illumina HiSeq2500 (Genomics Core Facility, Princeton, NJ, USA) or using NEBNext
417 Ultra RNA Library Preparation Lit (NEB) and sequenced on Illumina HiSeq4000 (Genewiz, South
418 Plainfield, NJ, USA) (Table S2). All raw RNA-seq data generated for this study have been deposited
419 in the National Center for Biotechnology Information (NCBI) Sequence Read Archive (SRA) under
420 bioproject PRJNA754197. Together with SRA datasets downloaded from public database, reads
421 were trimmed to Phred quality ≥ 20 and length ≥ 20 and then assembled *de novo* using Trinity
422 v2.2.0 (43). Sequences of ATP1A paralogs 1, 2 and 3 were pulled out with BLAST searches (blast-
423 v2.26), individually curated, and then aligned using ClustalW. Complete alignments of ATP1/2/3
424 can be found in Supplementary Dataset 1.

425

426 **Character state mapping and parameter estimation for the ATP1A1-3 paralogs**

427 Protein sequences from ATP1A1 (N=429), ATP1A2 (N=197) and ATP1A3 (N=205) including main
428 tetrapod groups (amphibians, non-avian reptiles, birds, and mammals) and lungfish+coelacanth as
429 outgroups were aligned using ClustalW with default parameters. The optimal parameters for
430 phylogenetic reconstruction were taken from the best-fit amino acid substitution model based on
431 Akaike Information Criterion (AIC) as implemented in ModelTest-NG v.0.1.5 (44), and was inferred
432 to be JTT+G4+F. An initial phylogeny was inferred using RAxML HPC v.8 (45) under the
433 JTT+GAMMA model with empirical amino acid frequencies. Branch lengths and node support

434 (aLRS) were further refined using PhyML v.3.1 (46) with empirical amino acid frequencies and
435 maximum likelihood estimates of rate heterogeneity parameters, I and $\Gamma$. Phylogeny visualization
436 and mapping of character states for each paralog was done using the R package ggtree (47).
437
438 **Ancestral sequence reconstruction and convergence calculations**
439 Ancestral sequence reconstruction (ASR) was performed in PAML using codeml (48) under the
440 JTT+G4+F substitution model. Statistical confidence in each position's reconstructed state for each
441 ancestor was determined from the posterior probability (PP), and only states with PP>0.8 were
442 considered. Ancestral sequences from all nodes in the ATP1A phylogeny were retrieved from the
443 codeml output, resulting in an alignment of 1,660 ATP1A proteins (831 extant species and 829
444 inferred ancestral sequences; Fig. S1). For each branch in the tree, we determined the occurrence
445 of substitutions by using the ancestral and derived amino acid states at each site using only states
446 with PP>0.8. All branch pairs were compared, except sister branches and ancestor-descendent
447 pairs (12, 13). When comparing substitutions on two distinct branches at the same site,
448 substitutions to the same amino acid state were counted as convergences, while substitutions away
449 from a common amino acid were counted as divergences. An alignment of 1,040 amino acids was
450 used to calculate the number of molecular convergences and divergences, excluding a putative 30
451 amino acid-long alternative spliced region (positions 834-864). Model-based estimates of sequence
452 divergence, number of convergences, number of divergences, and total number of substitutions
453 since the common ancestor were recorded for each pairwise comparison. We calculated the
454 proportion of observed convergent events per branch as (number of convergences +1) / (number
455 of divergences +1). The line describing the trend was calculated as a running average with window
456 size of 0.05 substitutions/site. 95% confidence intervals were calculated based on 100 bootstrap
457 replicates per window, resampling only variable sites.
458
459 For sites 111 and 122, molecular convergence was coded as "1" when the substitution along
460 $branch_i$ was to the same amino acid state as the substitution along $branch_j$, and "0" if substitutions
461 were to different states. Model-based estimates of sequence divergence, amino acid state, and
462 convergence event were recorded for each pairwise comparison (when convergence was "0",
463 amino acid state was set to "NA"). A logistic regression between molecular convergence (0 or 1)
464 and genetic distance was used to test for the correlation between variables (Fig 6B; Fig. S3)
465
466 **Construction of expression vectors**.
467 ATP1A1 and ATP1B1 wild-type sequences for the eight selected tetrapod species (Fig 4) were
468 synthesized by Invitrogen™ GeneArt. The $\beta$1-subunit genes were inserted into pFastBac Dual
469 expression vectors (Life Technologies) at the p10 promoter with XhoI and PaeI (FastDigest Thermo

470 Scientific™) and then control sequenced. The α1-subunit genes were inserted at the PH promoter
471 of vectors already containing the corresponding $\beta$1-subunit proteins using In-Fusion® HD Cloning
472 Kit (Takara Bio, USA Inc.) and control sequenced. All resulting vectors had the α1-subunit gene
473 under the control of the PH promoter and a $\beta$1-subunit gene under the p10 promoter. The resulting
474 eight vectors were then subjected to site-directed mutagenesis (QuickChange II XL Kit; Agilent
475 Technologies, La Jolla, CA, USA) to introduce the codons of interest. In total, 21 vectors were
476 produced (Table S3).
477
478 **Generation of recombinant viruses and transfection into Sf9 cells.**
479 *Escherichia coli* DH10bac cells harboring the baculovirus genome (bacmid) and a transposition
480 helper vector (Life Technologies) were transformed according to the manufacturer's protocol with
481 expression vectors containing the different gene constructs. Recombinant bacmids were selected
482 through PCR screening, grown, and isolated. Subsequently, Sf9 cells (4 x $10^5$ cells*ml) in 2 ml of
483 Insect-Xpress medium (Lonza, Walkersville, MD, USA) were transfected with recombinant bacmids
484 using Cellfectin reagent (Life Technologies). After a three-day incubation period, recombinant
485 baculoviruses were isolated (P1) and used to infect fresh Sf9 cells (1.2 x $10^6$ cells*ml) in 10 ml of
486 Insect-Xpress medium (Lonza, Walkersville, MD, USA) with 15 mg/ml gentamycin (Roth, Karlsruhe,
487 Germany) at a multiplicity of infection of 0.1. Five days after infection, the amplified viruses were
488 harvested (P2 stock).
489
490 **Preparation of Sf9 membranes.**
491 For production of recombinant NKA, Sf9 cells were infected with the P2 viral stock at a multiplicity
492 of infection of $10^3$. The cells (1.6 x $10^6$ cells*ml) were grown in 50 ml of Insect-Xpress medium
493 (Lonza, Walkersville, MD, USA) with 15 mg/ml gentamycin (Roth, Karlsruhe, Germany) at 27°C in
494 500 ml flasks (35). After 3 days, Sf9 cells were harvested by centrifugation at 20,000 x g for 10 min.
495 The cells were stored at -80 °C and then resuspended at 0 °C in 15 ml of homogenization buffer
496 (0.25 M sucrose, 2 mM EDTA, and 25 mM HEPES/Tris; pH 7.0). The resuspended cells were
497 sonicated at 60 W (Bandelin Electronic Company, Berlin, Germany) for three 45 s intervals at 0 °C.
498 The cell suspension was then subjected to centrifugation for 30 min at 10,000 x g (J2-21 centrifuge,
499 Beckmann-Coulter, Krefeld, Germany). The supernatant was collected and further centrifuged for
500 60 m at 100,000 x g at 4 °C (Ultra- Centrifuge L-80, Beckmann-Coulter) to pellet the cell
501 membranes. The pelleted membranes were washed once and resuspended in ROTIPURAN® p.a.,
502 ACS water (Roth) and stored at -20 °C. Protein concentrations were determined by Bradford assays
503 using bovine serum albumin as a standard. Three biological replicates were produced for each
504 NKA construct.
505

506 **Verification by SDS-PAGE/western blotting.**

507 For each biological replicate, 10 μg of protein were solubilized in 4x SDS-polyacrylamide gel
508 electrophoresis sample buffer and separated on SDS gels containing 10% acrylamide.
509 Subsequently, they were blotted on nitrocellulose membrane (HP42.1, Roth). To block non-specific
510 binding sites after blotting, the membrane was incubated with 5% dried milk in TBS-Tween 20 for
511 1 h. After blocking, the membranes were incubated overnight at 4 °C with the primary monoclonal
512 antibody α5 (Developmental Studies Hybridoma Bank, University of Iowa, Iowa City, IA, USA).
513 Since only membrane proteins were isolated from transfected cells, detection of the α subunit also
514 indicates the presence of the β subunit. The primary antibody was detected using a goat-anti-
515 mouse secondary antibody conjugated with horseradish peroxidase (Dianova, Hamburg,
516 Germany). The staining of the precipitated polypeptide-antibody complexes was performed by
517 addition of 60 mg 4-chloro-1 naphtol (Sigma-Aldrich, Taufkirchen, Germany) in 20 ml ice-cold
518 methanol to 100 ml phosphate buffered saline (PBS) containing 60 μl 30% $H_2O_2$. See Fig. S6.

519

520 **Ouabain inhibition assay.**

521 To determine the sensitivity of each NKA construct against cardiotonic steroids (CTS), we used the
522 water-soluble cardiac glycoside, ouabain (Acrōs Organics), as our representative CTS. 100 ug of
523 each protein was pipetted into each well in a nine-well row on a 96-well microplate (Fisherbrand)
524 containing stabilizing buffers (see buffer formulas in (49)). Each well in the nine-well row was
525 exposed to exponentially decreasing concentrations ($10^{-3}$ M, $10^{-4}$ M, $10^{-5}$ M, $10^{-6}$ M, $10^{-7}$ M, $10^{-8}$ M,
526 dissolved in distilled $H_2O$) of ouabain, distilled water only (experimental control), and a combination
527 of an inhibition buffer lacking KCl and $10^{-2}$ M ouabain to measure background protein activity (49).
528 The proteins were incubated at 37°C and 200 rpms for 10 minutes on a microplate shaker
529 (Quantifoil Instruments, Jena, Germany). Next, ATP (Sigma Aldrich) was added to each well and
530 the proteins were incubated again at 37°C and 200 rpms for 20 minutes. The activity of NKA
531 following ouabain exposure was determined by quantification of inorganic phosphate (Pi) released
532 from enzymatically hydrolyzed ATP. Reaction Pi levels were measured according to the procedure
533 described in Taussky and Shorr (50) (see Petschenka et al. (49)). All assays were run in duplicate
534 and the average of the two technical replicates was used for subsequent statistical analyses.
535 Absorbance for each well was measured at 650 nm with a plate absorbance reader (BioRad Model
536 680 spectrophotometer and software package). See Table S4.

537

538 **ATP hydrolysis assay.**

539 To determine the functional efficiency of different NKA constructs, we calculated the amount of Pi
540 hydrolyzed from ATP per mg of protein per minute. The measurements were obtained from the
541 same assay as described above. In brief, absorbance from the experimental control reactions, in

which 100 μg of protein was incubated without any inhibiting factors (i.e., ouabain or buffer excluding KCl), were measured and translated to mM Pi from a standard curve that was run in parallel (1.2 mM Pi, 1 mM Pi, 0.8 mM Pi, 0.6 mM Pi, 0.4 mM Pi, 0.2 mM Pi, 0 mM Pi). See Table S4.

**Statistical analyses of functional data.**

Background phosphate absorbance levels from reactions with inhibiting factors were used to calibrate phosphate absorbance in wells measuring ouabain inhibition and in the control wells measuring non-inhibited NKA activity (49). For ouabain sensitivity measurements, calibrated absorbance values were converted to percentage non-inhibited NKA activity based on measurements from the control wells (49). These data were plotted and log $IC_{50}$ values were obtained for each biological replicate from nonlinear fitting using a four-parameter logistic curve, with the top asymptote set to 100 and the bottom asymptote set to zero. Curve fitting was performed with the nlsLM function of the minipack.lm library in R. For comparisons of recombinant protein activity, the calculated Pi concentrations of 100 μg of protein assayed in the absence of ouabain were converted to nmol Pi/mg protein/min. $IC_{50}$ values were log-transformed. We used pairwise *t*-tests with Bonferroni corrections to identify significant differences between constructs with and without engineered substitutions. We used a two-way ANOVA to test for background dependence of substitutions (i.e., interaction between background and amino acid substitution) with respect to ouabain resistance (log $IC_{50}$) and protein activity. Specifically, we tested whether the effects of a substitution X->Y are equal on different backgrounds (null hypothesis: X->Y (background 1) = X->Y (background 2)). We further assumed that the effects of a substitution X->Y should exactly match that of Y->X. All statistical analyses were implemented in R. Data were plotted using the ggplot2 package in R.

**Acknowledgments**

We thank C. Natarajan, P. Kowalski, M. Winter, and V. Wagschal for assistance in the laboratory, and D.A. Gómez-Sánchez for assistance in the field. We thank J. Oaks for providing tissue from ring-necked snake. **Funding:** This study was funded by grants from the National Institutes of Health to PA (R01-GM115523), JFS (R01-HL087216) and SM (F32–HL149172), the National Science Foundation (OIA-1736249) to JFS, the Deutsche Forschungsgemeinschaft (Do 517/10-1) to SD, and the Alexander von Humboldt Foundation to SM.

580 **References**
581


582 1. D. L. Stern, The genetic causes of convergent evolution. *Nat. Rev. Genet.* **14**, 751–764
583 (2013).

584 2. J. F. Storz, Causes of molecular convergence and parallelism in protein evolution. *Nat. Rev.*
585 *Genet.* **17**, 239 (2016).

586 3. D. L. Stern, *Evolution, development, & the predictable genome* (Roberts and Co. Publishers,
587 2011).

588 4. P. C. Phillips, Epistasis—the essential role of gene interactions in the structure and
589 evolution of genetic systems. *Nat. Rev. Genet.* **9**, 855–867 (2008).

590 5. W. Fitch, Rate of change of concomitantly variable codons. *J. Mol. Evol.* **1**, 84–96 (1971).

591 6. B. Callahan, R. A. Neher, D. Bachtrog, P. Andolfatto, B. I. Shraiman, Correlated evolution of
592 nearby residues in Drosophilid proteins. *PLoS Genet.* **7**, e1001315 (2011).

593 7. T. N. Starr, J. W. Thornton, Epistasis in protein evolution. *Protein Sci.* **25**, 1204–1218
594 (2016).

595 8. J. F. Storz, Compensatory mutations and epistasis for protein function. *Curr. Opin. Struct.*
596 *Biol.* **50**, 18–25 (2018).

597 9. D. D. Pollock, G. Thiltgen, R. A. Goldstein, Amino acid coevolution induces an evolutionary
598 Stokes shift. *Proc. Natl. Acad. Sci.* **109**, E1352 (2012).

599 10. P. Shah, D. M. McCandlish, J. B. Plotkin, Contingency and entrenchment in protein
600 evolution under purifying selection. *Proc. Natl. Acad. Sci.* **112**, E3226 (2015).

601 11. V. O. Pokusaeva, *et al.*, An experimental assay of the interactions of amino acids from
602 orthologous sequences shaping a complex fitness landscape. *PLoS Genet.* **15**, e1008079
603 (2019).

604 12. R. A. Goldstein, S. T. Pollard, S. D. Shah, D. D. Pollock, Nonadaptive amino acid
605 convergence rates decrease over time. *Mol. Biol. Evol.* **32**, 1373–1381 (2015).

606 13. Z. Zou, J. Zhang, Are convergent and parallel amino acid substitutions in protein evolution
607 more prevalent than neutral expectations? *Mol. Biol. Evol.* **32**, 2085–2096 (2015).

608 14. Z. Zou, J. Zhang, Gene tree discordance does not explain away the temporal decline of
609 convergence in mammalian protein sequence evolution. *Mol. Biol. Evol.* **34**, 1682–1688
610 (2017).

611 15. J. B. Lingrel, The physiological significance of the cardiotonic steroid/ouabain-binding site
612 of the Na, K-ATPase. *Annu. Rev. Physiol.* **72**, 395–412 (2010).

613 16. A. Koksoy, Na+, K+-ATPase: a review. *J Ank. Med Sch* **24**, 73–82 (2002).

614 17. S. Dobler, S. Dalla, V. Wagschal, A. A. Agrawal, Community-wide convergent evolution in
615 insect adaptation to toxic cardenolides by substitutions in the Na, K-ATPase. *Proc. Natl.*
616 *Acad. Sci.* **109**, 13040–13045 (2012).

617 18. Y. Zhen, M. L. Aardema, E. M. Medina, M. Schumer, P. Andolfatto, Parallel molecular
618 evolution in an herbivore community. *Science* **337**, 1634–1637 (2012).

619 19. D. J. Moore, D. C. Halliday, D. M. Rowell, A. J. Robinson, J. S. Keogh, Positive Darwinian
620 selection results in resistance to cardioactive toxins in true toads (Anura: Bufonidae). *Biol.*
621 *Lett.* **5**, 513–516 (2009).

622 20. B. Ujvari, *et al.*, Widespread convergence in toxin resistance by predictable molecular
623 evolution. *Proc. Natl. Acad. Sci.* **112**, 11911–11916 (2015).

624 21. S. Mohammadi, *et al.*, Toxin-resistant isoforms of Na+/K+-ATPase in snakes do not closely
625 track dietary specialization on toads. *Proc. R. Soc. B Biol. Sci.* **283**, 20162111 (2016).

626 22. S. Mohammadi, L. Yang, M. Bulbert, H. M. Rowland, The evolutionary and behavioural
627 ecology of cardiotonic steroid resistance in predators (In prep).

628 23. A. M. Taverner, *et al.*, Adaptive substitutions underlying cardiac glycoside insensitivity in
629 insects exhibit epistasis in vivo. *eLife* **8**, e48224 (2019).

630 24. M. Karageorgi, *et al.*, Genome editing retraces the evolution of toxin resistance in the
631 monarch butterfly. *Nature* **574**, 409–412 (2019).

632 25. S. Mohammadi, *et al.*, Concerted evolution reveals co-adapted amino acid substitutions in
633 frogs that prey on toxic toads. *Curr. Biol.* **31**, 2530-2538.e10 (2021).

634 26. E. M. Price, J. B. Lingrel, Structure-function relationships in the sodium-potassium ATPase.
635 alpha. subunit: site-directed mutagenesis of glutamine-111 to arginine and asparagine-122
636 to aspartic acid generates a ouabain-resistant enzyme. *Biochemistry* **27**, 8400–8408
637 (1988).

638 27. K. J. Sweadner, *et al.*, Genotype-structure-phenotype relationships diverge in paralogs
639 ATP1A1, ATP1A2, and ATP1A3. *Neurol. Genet.* **5**, e303–e303 (2019).

640 28. A. Mobasheri, *et al.*, Na+, K+-ATPase isozyme diversity; comparative biochemistry and
641 physiological implications of novel functional interactions. *Biosci. Rep.* **20**, 51–91 (2000).

642 29. B. Ujvari, *et al.*, Isolation breeds naivety: island living robs Australian varanid lizards of
643 toad-toxin immunity via four-base-pair mutation. *Evol. Int. J. Org. Evol.* **67**, 289–294
644 (2013).

645 30. B. M. Marshall, *et al.*, Widespread vulnerability of Malagasy predators to the toxins of an
646 introduced toad. *Curr. Biol.* **28**, R654–R655 (2018).

647 31. S. Groen, N. Whiteman, Convergent evolution of cardiac-glycoside resistance in predators
648 and parasites of milkweed herbivores. *Curr. Biol.* **31**, R1465–R1466 (2021).

649 32. M. Lunzer, G. B. Golding, A. M. Dean, Pervasive cryptic epistasis in molecular evolution.
650 *PLoS Genet* **6**, e1001162 (2010).

651 33. L. Yang, *et al.*, Predictability in the evolution of Orthopteran cardenolide insensitivity.
652 *Philos. Trans. R. Soc. B* **374**, 20180246 (2019).

653 34. A. Stoltzfus, D. M. McCandlish, Mutational Biases Influence Parallel Adaptation. *Mol. Biol.*
654 *Evol.* **34**, 2163–2172 (2017).

655 35. J. Zhang, S. Kumar, Detection of convergent and parallel evolution at the amino acid
656 sequence level. *Mol. Biol. Evol.* **14**, 527–536 (1997).

657 36. L. F. Toledo, R. Ribeiro, C. F. Haddad, Anurans as prey: an exploratory analysis and size
658 relationships between predators and their prey. *J. Zool.* **271**, 170–177 (2007).

659 37. S. Dobler, *et al.*, New ways to acquire resistance: imperfect convergence in insect
660 adaptations to a potent plant toxin. *Proc. R. Soc. B* **286**, 20190883 (2019).

661 38. M. V. Clausen, F. Hilbers, H. Poulsen, The structure and function of the Na, K-ATPase
662 isoforms in health and disease. *Front. Physiol.* **8**, 371 (2017).

663 39. J. A. Wells, Additivity of mutational effects in proteins. *Biochemistry* **29**, 8509–8517 (1990).

664 40. M. Lunzer, S. P. Miller, R. Felsheim, A. M. Dean, The biochemical architecture of an ancient
665 adaptive landscape. *Science* **310**, 499–501 (2005).

666 41. L. I. Gong, M. A. Suchard, J. D. Bloom, Stability-mediated epistasis constrains the evolution
667 of an influenza protein. *Elife* **2**, e00631 (2013).

668 42. P. Nosil, *et al.*, Ecology shapes epistasis in a genotype–phenotype–fitness map for stick
669 insect colour. *Nat. Ecol. Evol.* **4**, 1673–1684 (2020).

670 43. B. J. Haas, *et al.*, De novo transcript sequence reconstruction from RNA-seq using the
671 Trinity platform for reference generation and analysis. *Nat. Protoc.* **8**, 1494–1512 (2013).

672 44. D. Darriba, *et al.*, ModelTest-NG: a new and scalable tool for the selection of DNA and
673 protein evolutionary models. *Mol. Biol. Evol.* **37**, 291–294 (2020).

674 45. A. Stamatakis, RAxML version 8: a tool for phylogenetic analysis and post-analysis of large
675 phylogenies. *Bioinformatics* **30**, 1312–1313 (2014).

676 46. S. Guindon, *et al.*, New algorithms and methods to estimate maximum-likelihood
677 phylogenies: assessing the performance of PhyML 3.0. *Syst. Biol.* **59**, 307–321 (2010).

678 47. G. Yu, D. K. Smith, H. Zhu, Y. Guan, T. T. Lam, ggtree: an R package for visualization and
679 annotation of phylogenetic trees with their covariates and other associated data. *Methods*
680 *Ecol. Evol.* **8**, 28–36 (2017).

681 48. Z. Yang, PAML 4: phylogenetic analysis by maximum likelihood. *Mol. Biol. Evol.* **24**, 1586–
682 1591 (2007).

683 49. G. Petschenka, *et al.*, Stepwise evolution of resistance to toxic cardenolides via genetic
684 substitutions in the Na+/K+-ATPase of milkweed butterflies (Lepidoptera: Danaini).
685 *Evolution* **67**, 2753–2761 (2013).

686 50. H. H. Taussky, E. Shorr, A microcolorimetric method for the determination of inorganic
687 phosphorus. *J. Biol. Chem.* **202**, 675–685 (1953).

688

689

690 **Figures and Tables**

691
692

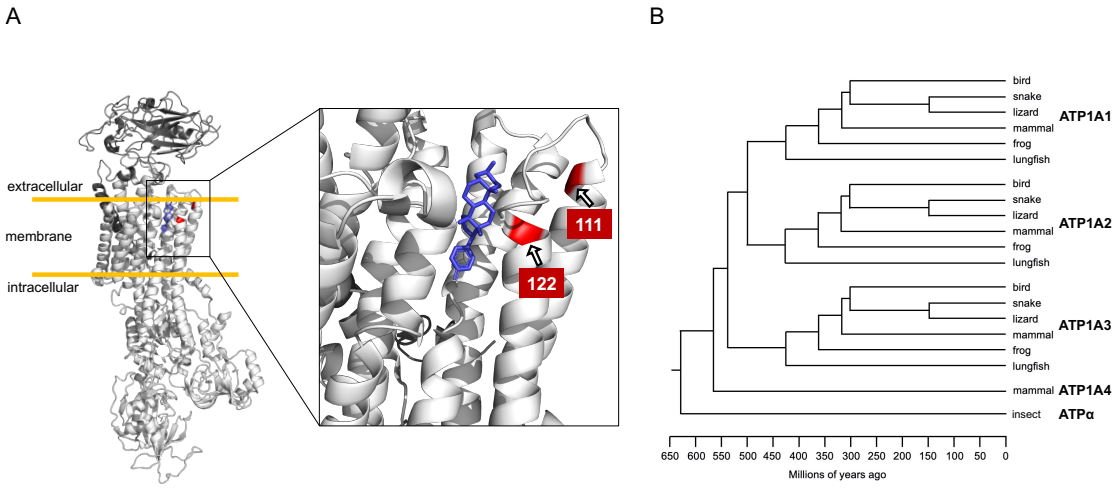


693

694 **Figure 1. $Na^+$,$K^+$-ATPase structure and phylogenetic relationships of ATP1A paralogs among**
695 **vertebrates.** (A) Crystal structure of an $Na^+$,$K^+$-ATPase (NKA) with a bound the representative CTS
696 bufalin in blue (PDB 4RES). The zoomed-in panel shows the H1-H2 extracellular loop, highlighting
697 two amino acid positions (111 and 122 in red) that have been implicated repeatedly in CTS
698 resistance. We highlight key examples of convergence in amino acid substitutions at sites in the
699 H1-H2 extracellular loop associated with CTS resistance in Fig 3. (B) Phylogenetic relationships
700 among ATP1A paralogs of vertebrates and ATP$\alpha$ of insects.
701

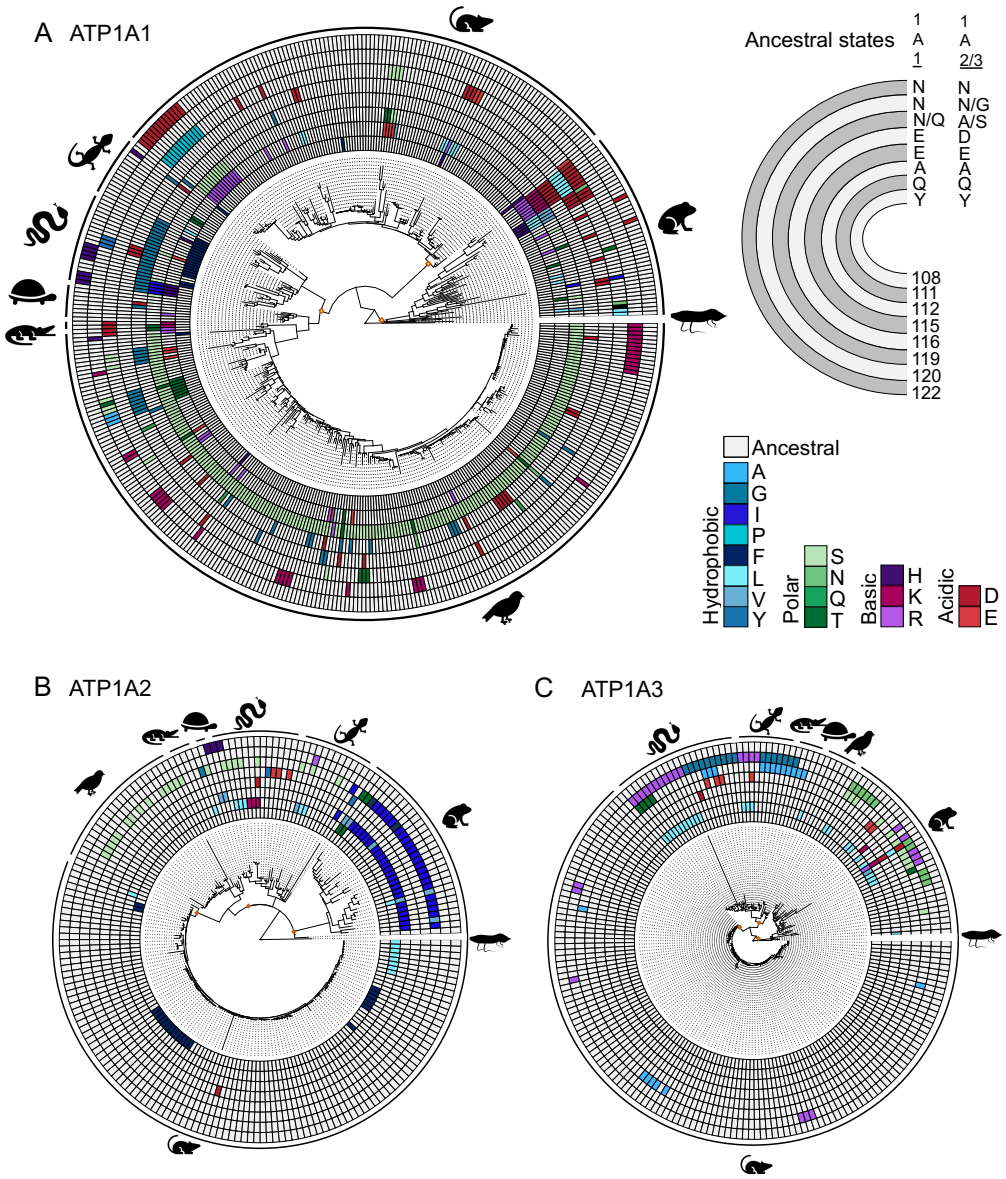


**Figure 2. Patterns of molecular evolution in the α(M1–M2) extracellular loop of ATP1A paralogs shared among tetrapods.** (A) Maximum likelihood phylogeny of tetrapod ATP1A1, (B) ATP1A2, and (C) ATP1A3. The character states for eight sites relevant to CTS resistance in and near the H1-H2 loop of the NKA protein are shown at the node tips. Yellow internal nodes indicate ancestral sequences reconstructed to infer derived amino acid states across clades to ease visualization; nodes reconstructed: MRCA of mammals, reptiles, and amphibians. *Top right*, each semi-circle indicates the site mapped in the main phylogeny with the inferred ancestral amino acid state for each of the three yellow nodes (posterior probability >0.8). In ATP1A1, site 119 was inferred as Q119 for amphibians and mammals, and N119 for reptiles (Table S6); in ATP1A2-3 site 119 was inferred as A119 for amphibians and reptiles, and S119 for mammals (Table S6). Site number corresponds to pig (*Sus scrofa*) reference sequence. Higher number and variation of substitutions in ATP1A1 stand out in comparison to the other paralogs.

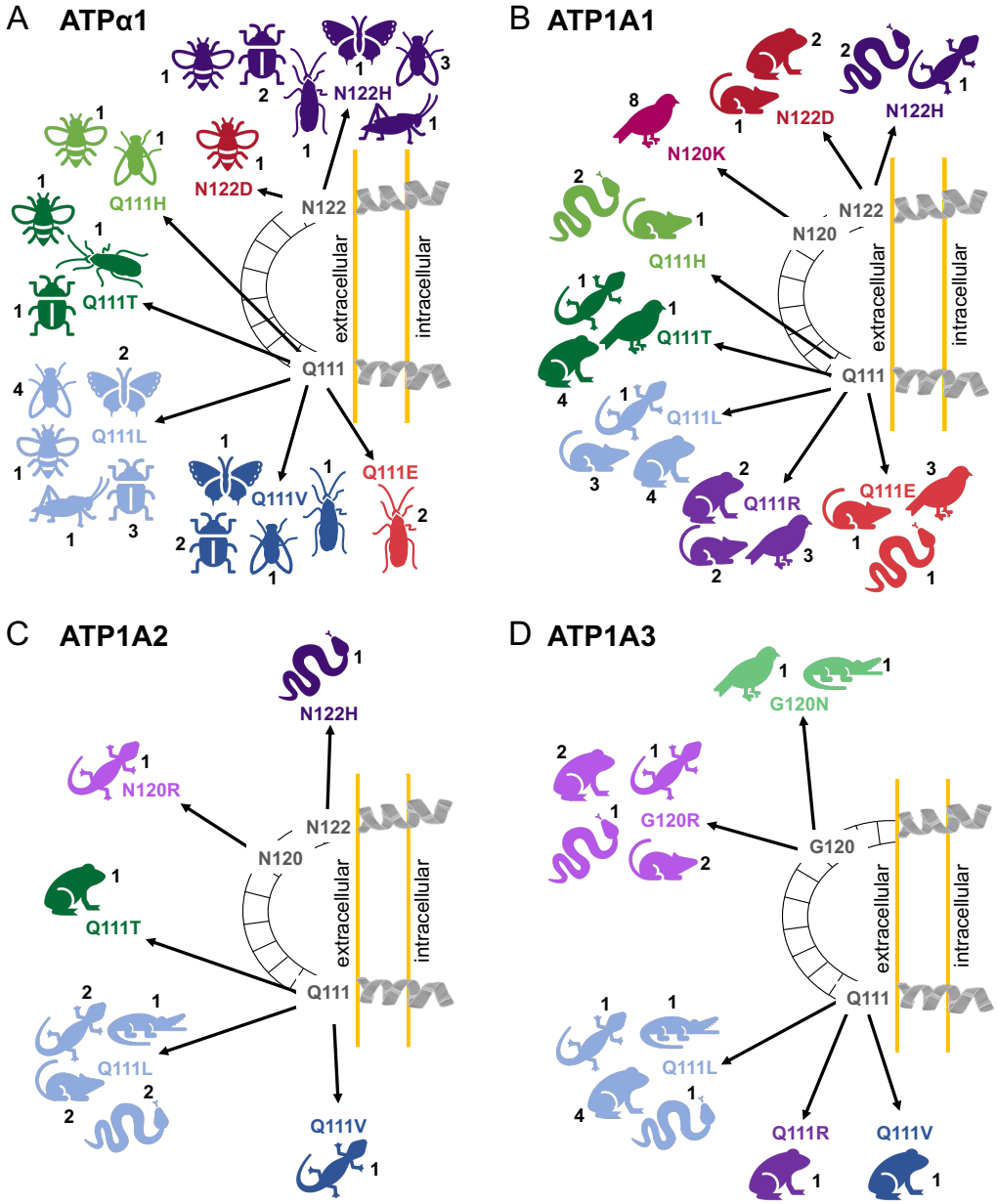


**Figure 3. Parallel and divergent patterns of CTS-resistant substitutions across ATPα1 of insects and the shared ATP1A paralogs of tetrapods.** Examples of convergence in ATPα1 across insects (A). Convergence in the **(B)** ATP1A1, **(C)** ATP1A2, and **(D)** ATP1A3 paralogs, respectively, across tetrapods. Numbers indicate the number of independent substitutions in each major clade depicted. For ATP1A3, resistance-conferring amino acid substitutions have been identified at site 120, and not 122. A full list of amino acid substitutions can be found in Supplementary Dataset 2 for tetrapods, and Taverner et al. (23) for insects.

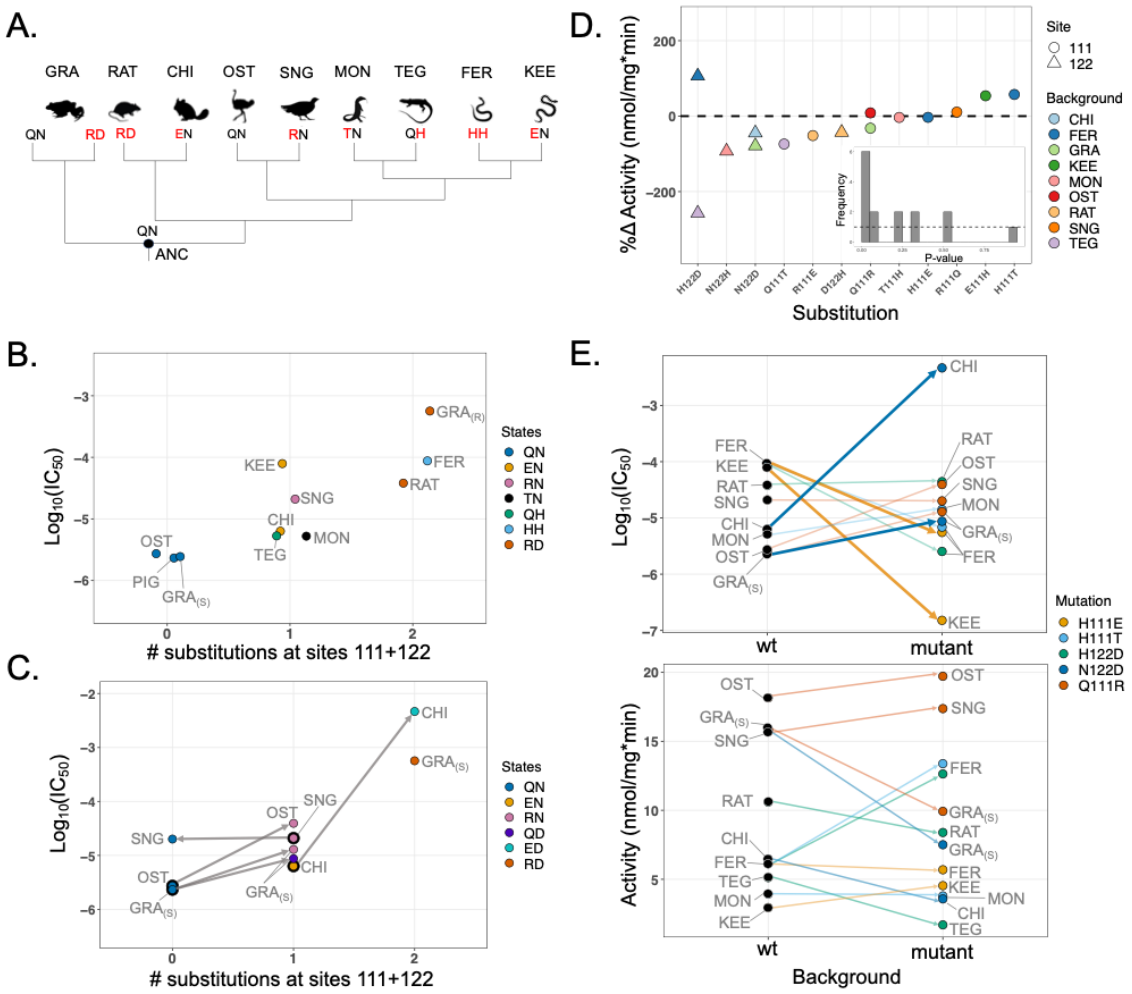


**Figure 4. Functional properties of wild-type and engineered ATP1A1**. **(A)** Cladogram relating the surveyed species. GRA: Grass Frog (*Leptodactylus*); RAT: Rat (*Rattus*); CHI: Chinchilla (*Chinchilla*); OST: Ostrich (*Struthio*); SNG: Sandgrouse (*Pterocles*); MON: Monitor lizard (*Varanus*); TEG: Tegu lizard (*Tupinambis*); FER: False fer-de-lance (*Xenodon*); KEE: Red-necked keelback snake (*Rhabdophis*). Two-letter codes underneath each avatar indicate native amino acid states at sites 111 and 122, respectively. Data for grass frog from Mohammadi et al. (2021). **(B)** Levels of CTS resistance (IC50) among wild-type enzymes. The x-axis distinguishes among ATP1A1 with 0, 1 or 2 derived states at sites 111 and 122. The subscripts S and R refer to the CTS-sensitive and CTS-resistant paralogs, respectively. **(C)** Effects of changing the number of substitutions at 111 or 122 on CTS resistance (IC50). Substitutions result in predictable changes to resistance except in the reversal R111Q in Sandgrouse (SNG). $GRA_S$ represents Q111R+N122D on the sensitive paralog background. **(D)** Effects of single substitutions on $Na^+$,$K^+$-ATPase (NKA) activity. Each modified ATP1A1 is compared to the wild-type enzyme for that species. The inset shows the distribution of *t*-test p-values for all 15 substitutions, with the dotted line indicating the expectation**. (E)** Evidence for epistasis for CTS resistance (IC50, upper panel) and lack of such effects for enzyme activity (lower panel). Each line compares the same substitution (or the reverse substitution) tested on at least two backgrounds. Thicker lines correspond to substitutions with significant sequence-context dependent effects (Bonferroni-corrected ANOVA p-values < 0.05, Table S5).

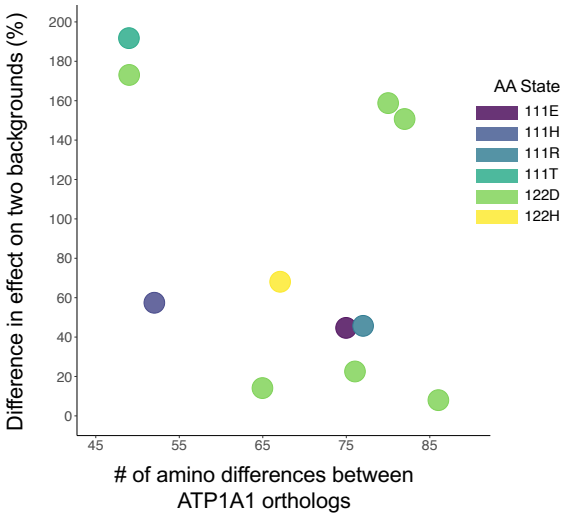


**Figure 5. No relationship between the effect of substitution to a given amino state on activity and the extent of divergence between ATP1A1 orthologs.** Each point represents a comparison between the effect (% change in activity relative to the wild-type enzyme) of a given amino acid state (e.g., 122D) on two different genetic backgrounds. For example, the effect of 122D between chinchilla and false fer-de-lance is measured as % change [chinchilla vs. chinchilla+N122D] minus the % change [false fer-de-lance vs. false fer-de-lance+H122D]. Comparisons were measured as the difference between the two effects. In total, 11 comparisons were possible. The x-axis represents the number of amino acid differences between two ATP1A1 proteins being compared. Assuming intramolecular epistasis for protein function is prevalent, a positive correlation is predicted. However, no such relationship is observed (Spearman's correlation, $r_S = -0.42$, $p = 0.19$).

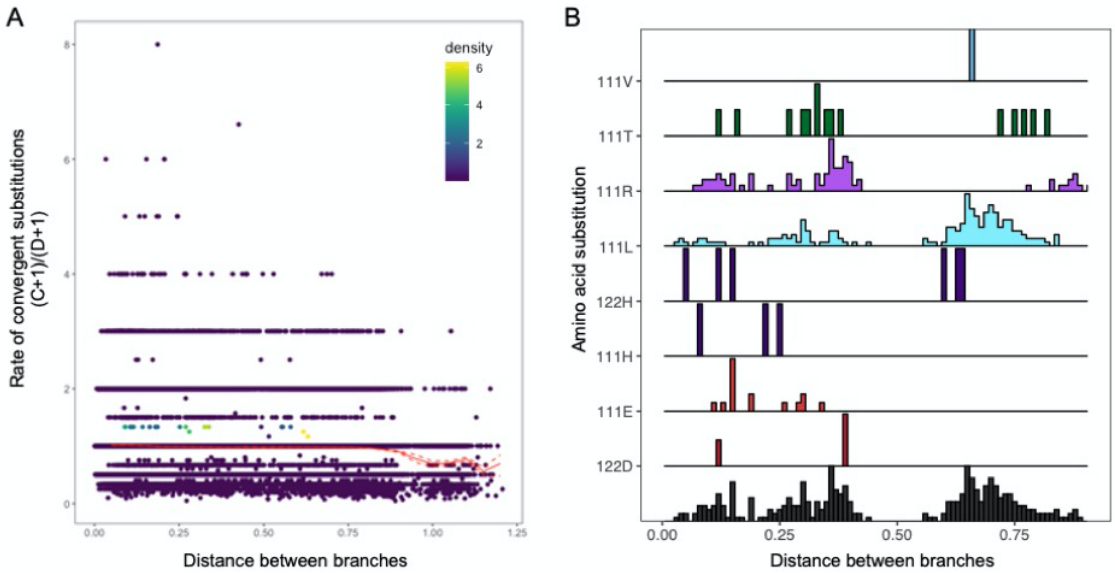


**Figure 6. Rate of convergence across ATP1A sequences as a function of increasing sequence divergence. (A)** Change in the rate of convergence (protein wide) over time for the ATP1A protein family. The proportion of convergent (C) over divergent (D) substitutions along the entire protein sequence was estimated for all pairs of branches in the ATP1A phylogeny, except for sister branches or ancestor-descendant pairs. Color scale shows the density of dots for both axes. The distance between branches corresponds to the expected number of amino acid substitutions per site between protein pairs being compared (under the JTT+G4+F model). The red line shows a running average with a window size of 0.05 substitutions/site. Dashed lines show the 95% confidence interval based on 100 bootstrap replicates per window. **(B)** For each derived amino acid state at sites 111 and 122, the histograms show the distribution of pairwise convergent events along the sequence divergence axis (expected number of substitutions per site). Substitutions are color coded as in Figure 2. The histogram at the bottom shows the combined distribution of pairwise convergent events for both sites.